Available online at www.sciencedirect.com
SCIENCE DIRECT®
Biochemical and Biophysical Research Communications 337 (2005) 720–729
BBRC
www.elsevier.com/locate/ybbrc

In vivo functional characterization of the SARS-Coronavirus 3a protein in *Drosophila* ☆

S.L. Alan Wong [a,b], Yiwei Chen [a,b], Chak Ming Chan [a,b], C.S. Michael Chan [a,b], Paul K.S. Chan [c], Y.L. Chui [d], Kwok Pui Fung [b,e], Mary M.Y. Waye [b,e], Stephen K.W. Tsui [b,e], H.Y. Edwin Chan [a,b,*]

[a] *Laboratory of Drosophila Research, The Chinese University of Hong Kong, Shatin, N.T., Hong Kong SAR, China*
[b] *Department of Biochemistry, The Chinese University of Hong Kong, Shatin, N.T., Hong Kong SAR, China*
[c] *Department of Microbiology, The Chinese University of Hong Kong, Shatin, N.T., Hong Kong SAR, China*
[d] *Clinical Immunology Unit, The Chinese University of Hong Kong, Shatin, N.T., Hong Kong SAR, China*
[e] *Croucher Laboratory for Human Genomics, The Chinese University of Hong Kong, Shatin, N.T., Hong Kong SAR, China*

Received 13 September 2005
Available online 26 September 2005

Abstract

The Severe Acute Respiratory Syndrome-Coronavirus (SARS-CoV) *3a* locus encodes a 274 a.a. novel protein, and its expression has been confirmed in SARS patients. To study functional roles of *3a*, we established a transgenic fly model for the SARS-CoV *3a* gene. Misexpression of *3a* in *Drosophila* caused a dominant rough eye phenotype. Using a specific monoclonal antibody, we demonstrated that the 3a protein displayed a punctate cytoplasmic localization in *Drosophila* as in SARS-CoV-infected cells. We provide genetic evidence to support that *3a* is functionally related to clathrin-mediated endocytosis. We further found that *3a* misexpression induces apoptosis, which could be modulated by cellular cytochrome c levels and caspase activity. From a forward genetic screen, 78 dominant *3a* modifying loci were recovered and the identity of these modifiers revealed that the severity of the 3*a*-induced rough eye phenotype depends on multiple cellular processes including gene transcriptional regulation.

Keywords: *Drosophila*; Genetic screen; Transgenics; U274; X1

The Severe Acute Respiratory Syndrome-Coronavirus (SARS-CoV) is a newly evolved coronavirus and is ascertained to be the etiological agent of the global atypical pneumonia pandemic in 2003. The SARS-CoV genome carries genes for the replicase enzymes, structural proteins, and several putative open reading frames (ORFs) with poorly defined functions [1,2]. The *3a* locus (also known as X1 [2], ORF3 [1], and U274 [3]) is unique to SARS-CoV and encodes a 274 a.a. novel protein. The 3a protein lacks sequence homology to any known proteins, but is predicted to carry three transmembrane domains and a C-terminal calcium-binding region [3–6]. The detection of 3a protein [5] and 3a-specific IgG antibodies [6–9] in SARS patients confirmed the cellular expression of 3a in SARS-CoV-infected cells and patients. The 3a protein localized preferentially on the Golgi apparatus in both transfected [5,10] and SARS-CoV-infected cells [5]. In addition, 3a was also detected on the plasma membrane [3,11]. Recent findings revealed that 3a interacted physically with other SARS-CoV structural proteins, including spike (S), membrane, and envelope [3,6], and was also detected in newly packaged matured SARS-CoV virions [11,12]. These findings would therefore imply that 3a functions as both a viral

☆ *Abbreviations:* a.a., amino acid; AO, acridine orange; Csp, cysteine string protein; *dc3*, *cytochrome-c-distal*; *emc*, *extra macrochaetae*; SARS-CoV, severe acute respiratory syndrome-Coronavirus; TfR, transferrin receptor.

* Corresponding author. Fax: +852 2603 7732.
E-mail address: hyechan@cuhk.edu.hk (H.Y.E. Chan).

0006-291X/$ - see front matter © 2005 Elsevier Inc. All rights reserved.
doi:10.1016/j.bbrc.2005.09.098

regulatory protein in infected cells and a structural protein in matured viral particles.

Many cellular proteins possess tyrosine-based YXXΦ motifs, which are sorting signals for internalization of proteins via endocytosis from the cell surface [13]. A functional YXXΦ signal has been identified in the porcine coronavirus but not SARS-CoV S protein [14]. On the other hand, 3a carries an analogous YXXΦ motif (160–163 a.a.) and it has also been reported to mediate protein internalization in cultured cells [3]. Because of the physical interaction between S and 3a [6], and the absence of an YXXΦ motif in the SARS-CoV S protein, it has therefore been hypothesized that one intracellular role of 3a is to modulate intracellular trafficking of S in SARS-CoV-infected cells [15].

Drosophila has been used to study the molecular functions of various viral gene products [16–18]. For example, the HIV-1 Tat protein was first found to interact with tubulin in *Drosophila* [16] and such interaction has subsequently been demonstrated in mammalian cells [19]. Therefore, *Drosophila* would be a feasible model to define intracellular regulatory actions of individual viral gene products [20]. Here, we established and characterized a *3a* transgenic fly model to elucidate the cellular regulatory actions of SARS-CoV *3a* locus in vivo. In brief, *3a* misexpression caused a dominant rough eye phenotype, and we showed that genes which mediate clathrin-dependent endocytosis dominantly suppressed the *3a*-induced rough eye phenotype. Furthermore, *3a* misexpression caused apoptosis. From a forward genetic screen, we further found that *3a* interacts genetically with genes that are involved in multiple cellular processes including gene transcription. In summary, our findings not only provide clues on the intracellular functions of *3a*, but also demonstrate the feasibility of transgenic fly models in the studies of SARS-CoV *3a* and other viral gene functions.

Materials and methods

Drosophila genetics. Fly strains were grown at 29 °C on standard cornmeal medium supplemented with dry yeast. The following fly lines were used in this study: *gmr-GAL4*; *34B-GAL4*; *UAS-DIAP1*; *UAS-emc* (a kind gift of J. de Celis); *UAS-GFP-lacZ*; *UAS-HSPA1L*; *UAS-P35*; *UAS-reaper*; *gmr-reaper*; Csp^{R1} (a kind gift of K. Zinsmaier); $CtBP^{87De\text{-}10}$; $dc3^{EP2305}$; $Eps15^{EP2513}$; lwr^{02858} (Bloomington *Drosophila* Stock Center); $Nedd4^{EY00500}$; $Su(H)^{EY07695}$ (Bloomington *Drosophila* Stock Center); the Exelixis and DrosDel deficiency collections.

Generation of 3a transgenic lines. The *3a* ORF was PCR amplified from viral cDNA to generate *pUAST-3a* and *pUAST-EGFP-3a* plasmids. The *UAS-3a* transgene produces a full-length non-tagged 3a protein, whereas the *UAS-EGFP-3a* transgene produces a full-length 3a protein with EGFP fused to its N-terminus. $UAS\text{-}EGFP\text{-}3a^{E0}$ and $UAS\text{-}3a^{F1}$ were selected for detailed analysis.

Genetic screen. We screened a total of 574 overlapping deletion lines to identify genomic regions that would modify the *EGFP-3a*-induced rough eye phenotype (Fig. 1B) when present in only one copy. Five hundred and one of the deletion lines are from the Exelixis collection, and 73 are from the DrosDel collection. A total of 93 deletion lines representing 24 genomic regions showed reproducible modification of the *EGFP-3a* phenotype.

Semi-quantitative RT-PCRs. Total RNA was prepared using Trizol reagent (Invitrogen). Primers used were dc3F: 5′ ATG GT TCT GGT GAT GCA 3′; dc3R: 5′ CTA CTT GTT TGA CTT GAG 3′; dc4F: 5′ ATG GGC GTT CCT GCT GGT 3′; dc4R: 5′ TTA CTT GT CGC CGA CTT 3′; emcF: 5′ TTC CGT TCA TGC CCA AGA ACA GGA 3′; emcR: 5′ GTT GGA CAG TTG CTG CTG TGA TTG 3′; GAPDHF: 5′ ACC GTC GAC GGT CCC TCT 3′; and GAPDHR: 5′ GTG TAG CCC AGG ATT CCC T 3′.

3a monoclonal antibodies. In brief, BALB/c mice were immunized intraperitoneally (i.p.) with 100 μg of the KLH-conjugated 3a peptide in complete Freund's adjuvant (Sigma–Aldrich), followed by monthly i.p. boosts using the same amount of antigen in incomplete Freund's adjuvant (Sigma–Aldrich). Preliminary screening of serum antibody activity and hybridoma fusion clones was determined by ELISA.

Western blot analysis. Primary antibodies used were anti-3a MAb X98 (1:40; this study), anti-cytochrome c clone 7H8.2C12 (1:500, Pharmingen), anti-Csp (1:50), and anti-β-tubulin E7 (1:2000; Developmental Studies Hybridoma Bank, Iowa City, IA, with funding from the NICHD).

Acridine orange staining and immunofluorescence. Acridine orange staining was performed as previously described [21]. Antibodies used for immunofluorescence include anti-3a MAbs X98 (1:20), anti-denatured cytochrome *c* clone 7H8.2C12 (1:200, Pharmingen), and anti-native cytochrome *c* clone 6H2.B2 (1:100; Pharmingen). Propidium iodide (PI) was used to label cell nuclei (Molecular Probes). Slides coated with both SARS-CoV-infected cells and non-infected cells were purchased from Euroimmun.

Results

To investigate *3a* function in vivo, the *3a* gene of the CUHK-W1 SARS-CoV isolate (AY278554) was used to generate *pUAST-EGFP-3a* and *pUAST-3a* constructs. When either *EGFP*- or non-tagged *3a* transgene was misexpressed in the *Drosophila* eye, a rough eye phenotype was observed (Fig. 1B and supplementary Fig. 2B). When misexpressed in the third instar larval eye imaginal disc and salivary gland cells, both EGFP-3a and non-tagged 3a proteins showed similar punctate cytoplasmic localizations (Figs. 1D and F, and supplementary Fig. 2D) as in SARS-CoV-infected cells (supplementary Fig. 1C). Since both *EGFP-3a* and *3a* transgenes showed comparable rough eye phenotype (Fig. 1B and supplementary Fig. 2B), *EGFP-3a* was mainly used in subsequent analyses.

Endocytosis and 3a function

A YXXΦ motif for rapid protein internalization has been identified in 3a [3], and similar sequences are also found in many cellular proteins, for example, the human transferrin receptor (TfR, [13]). It has been shown that internalization of TfR requires Eps15, an endocytic protein involved in clathrin-mediated endocytosis. When *EGFP-3a* was misexpressed in an *Eps15* mutant background [22], a dominant suppression of the *EGFP-3a*-induced rough eye phenotype was observed (Fig. 2C). Nedd4 is an E3 ubiquitin ligase and is able to monoubiquitinate Eps15 for its endocytic function [23]. We further found that a *P*-element insertion ($Nedd4^{EY00500}$) in the *Nedd4* gene also dominantly suppressed the *EGFP-3a*-induced rough eye phenotype (Fig. 2D). Our data support previous findings that *3a* is involved in protein trafficking [15], and our results highlight the involvement of clathrin-dependent endocytosis in *3a* function.

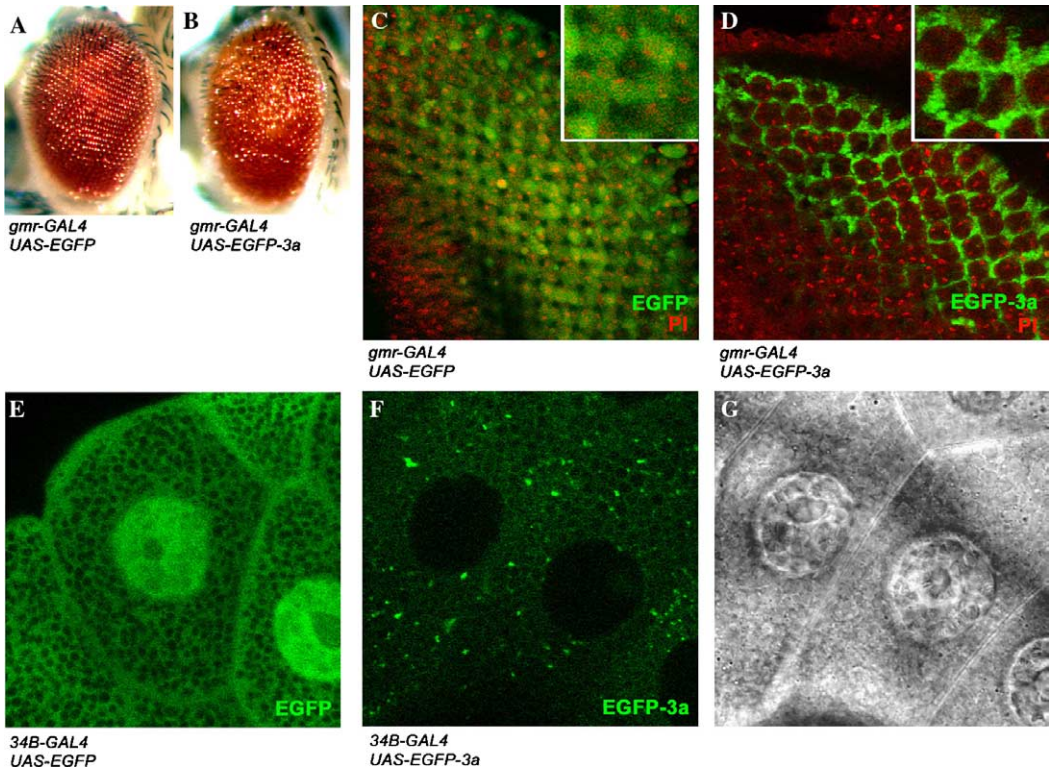

Fig. 1. Misexpression of the SARS-CoV *3a* gene in *Drosophila*. (A,B) Misexpression of the SARS-CoV *3a* gene caused external eye disruption in adult *Drosophila*. Misexpression of the control *EGFP* transgene (A) showed normal external eye morphology, whereas misexpression of the SARS-CoV *EGFP-3a* transgene (B) caused a rough eye phenotype as characterized by loss of regularity of the external eye structure. (C–G) Subcellular localization of the EGFP-3a fusion protein in *Drosophila*. Misexpression of the EGFP control protein showed homogeneous intracellular green fluorescence signals in both third instar eye imaginal disc (C) and salivary gland (E) cells. A distinct punctate cytoplasmic expression pattern of the EGFP-3a fusion protein was observed in both eye imaginal disc (D) and salivary gland cells (F). (G) Location of salivary gland cell nuclei of (F). Propidium iodide (PI) was used to stain cell nuclei in eye imaginal disc cells (C,D).

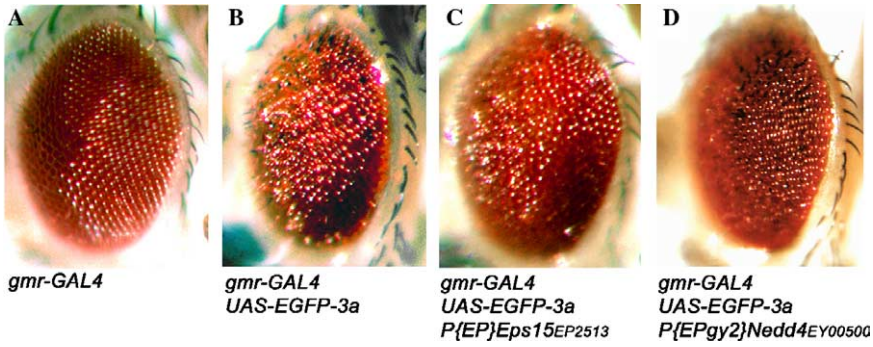

Fig. 2. Genes involved in endocytosis are related to the *EGFP-3a*-induced rough eye phenotype. Unlike the *gmr-GAL4* control (A), *EGFP-3a* misexpression resulted in a rough eye phenotype (B). A mutant allele of the endocytic gene *Eps15* ($Eps15^{EP2513}$) dominantly suppressed the *EGFP-3a*-induced rough eye phenotype (C). Nedd4 monoubiquitinates Eps15 and such modification is essential for *Eps15* function. A *P*-element insert line in the *Nedd4* locus ($Nedd4^{EY00500}$) showed dominant suppression of the *EGFP-3a* phenotype (D).

Misexpression of SARS 3a induces apoptosis in vivo

Apoptosis has been reported in SARS-CoV-infected cells [24–27]. We therefore investigated whether the *3a*-induced rough eye phenotype (Fig. 1B and supplementary Fig. 2B) was related to apoptotic cell death in flies. We performed acridine orange (AO) staining in third instar larval eye imaginal discs (Figs. 3G–M) and observed increased numbers of AO-positive apoptotic cells in *EGFP-3a*-expressing eye discs (Fig. 3J). Consistently, eye discs misexpressed with the non-tagged *3a* also showed increased numbers of AO-positive cells (supplementary Fig. 2F). When *EGFP-3a* was coexpressed with anti-apoptotic genes such as the caspase inhibitor *P*35, and the *Drosophila inhibitor of apoptosis 1* (*DIAP1*), the rough eye phenotype was mostly suppressed (Figs. 3E

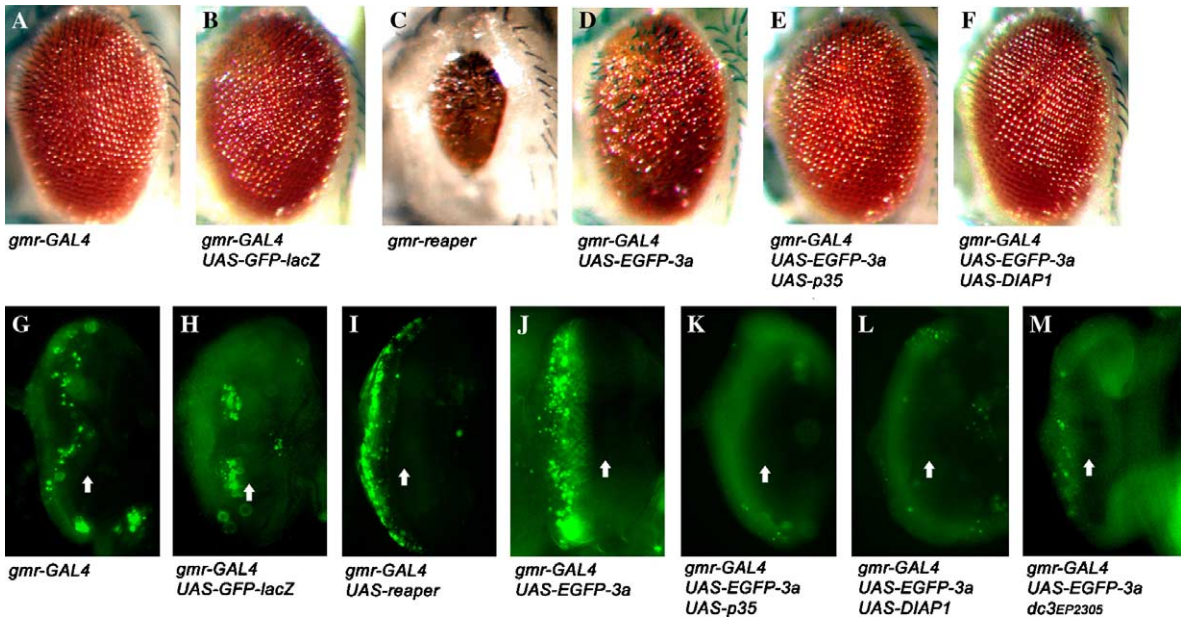

Fig. 3. Apoptotic pathway is related to the *EGFP-3a*-induced rough eye phenotype. (A–F) Overexpression of anti-apoptotic genes suppresses the *EGFP-3a*-induced rough eye phenotype. *gmr-GAL4* alone (A) and misexpression of EGFP-lacZ fusion protein by *gmr-GAL*4 (B) showed no external eye deformation. Overexpression of the pro-apoptotic gene *reaper* caused a rough eye phenotype and reduction in eye size (C). The *EGFP-3a*-induced rough eye phenotype (D) was suppressed when coexpressed with either *P*35 (E) or *DIAP1* (F). (G–M) Coexpression of anti-apoptotic genes reduces the number of apoptotic cells in third instar larval eye discs. Comparable numbers of acridine orange-positive apoptotic cells were observed in *gmr-GAL4* control eye discs (G) and discs misexpressed with a GFP-lacZ fusion protein (H). Expression of both *reaper* (I) and *EGFP-3a* (J) showed increased number of acridine orange-positive cells in eye discs. The *EGFP-3a*-induced apoptosis was suppressed by coexpression of baculoviral anti-apoptotic genes *P35* (K), *DIAP1* (L); and *cytochrome c dc3* (M). Arrows indicate the location of the morphological furrows.

and F). In addition, the number of AO-positive cells was also largely reduced when *P*35 or *DIAP1* was coexpressed with *EGFP-3a* (Figs. 3K and L). Our data therefore confirmed that the SARS-CoV *3a* gene is pro-apoptotic and its action can be counteracted by anti-apoptotic factors.

A genetic screen to define 3a functions in vivo

To further investigate the intracellular regulatory functions of *3a* in vivo, we initiated a forward genetic screen to identify genes that would modify the *EGFP-3a*-induced rough eye phenotype (Fig. 1B). Based on overlapping chromosomal deletions, 24 genomic regions were isolated (see experimental procedures). By crossing all mutant lines available at the Bloomington *Drosophila* Stock Center that fall into these 24 modifying genomic regions to *EGFP-3a* flies, 78 individual genes (represented by 99 mutant lines) showed reproducible modification of the *EGFP-3a*-induced rough eye phenotype. Forty-six of these modifier genes (~59%) have human orthologues and are also expressed in the human lung (http://www.ncbi.nlm.nih.gov/entrez/query.fcgi?db=unigene). Based on their cellular functions, most of the *EGFP-3a* modifiers were classified into 5 categories including electron transport, gene transcription, protein posttranslational modification, calcium-binding, and nucleic acid-binding. Nineteen modifying loci are discussed here (Table 1).

Cytochrome c dominantly modifies 3a-induced rough eye phenotype

One of the *3a* modifiers identified from our screen is *cytochrome c* (Fig. 4C). In *Drosophila*, there are 2 *cytochrome c* genes (*dc3* and *dc4*) and they are both located at the 36A10-B3 region (Fig. 4E). A deletion line *Df(2L)Exel6039*, which uncovers this region, dominantly enhanced the *EGFP-3a*-induced rough eye phenotype (Fig. 4C). We further showed that cytochrome c protein levels were significantly reduced in this deletion line (Fig. 4F). Conversely, overexpression of the endogenous *dc3* gene (Figs. 4G and H), by means of an EP insert line $dc3^{EP2305}$, dominantly suppressed the *EGFP-3a* phenotype (Fig. 4D). Our data therefore suggest that the severity of the *EGFP-3a*-induced rough eye phenotype correlates with cellular cytochrome c levels. In support of this, a reduction in the number of AO-positive cells was observed when *EGFP-3a* was coexpressed with $dc3^{EP2305}$ (Fig. 3M). Further, we showed that *EGFP-3a* overexpression did not affect mRNA expression levels of both *dc3* and *dc4* genes (Fig. 4G).

Transcriptional dysregulation in 3a flies

The C-terminal-binding-protein (CtBP) is a transcriptional corepressor protein. From our screen, we found that a chromosome deletion line (87D8-10) and a mutant allele

Table 1
19 loci that dominantly modify the *EGFP-3a*-induced rough eye phenotype

Category	Gene	Allele	Modification (Strength)[a]	Molecular function[b]	Human homologue[b]	Human lung expression[c]
Electron transport	Cyt-c-d (dc3)	*Cyt-c-d*^{EP2305}	Su(+)	Electron transporter activity; oxidoreductase activity; electron transporter, transferring electrons from CoQH2-cytochrome *c* reductase complex and cytochrome *c* oxidase complex activity	Cytochrome *c*, somatic (CYCS)	Yes
Calcium-binding	CalpB	*EP(3)875*	Su(++)	Calmodulin binding; calpain activity; calcium ion binding	Calpain 9 (CAN9)	Yes
	Csp	*EP(3)659*	Su(+)	ATPase activity, coupled	DnaJ (Hsp40) homolog, subfamily C, member5 (DNAJC5)	Yes
		EP(3)3141	Su(+)			
	Past1	*Past1*^{EY01852}	E(−)	Calmodulin binding; calcium ion binding	EH-domain containing 1 (EHD1)	Yes
Protein post-translational modification	lwr	*lwr*^{02858}	Su(+)	SUMO conjugating enzyme activity; ligase activity; protein binding; ubiquitin conjugating enzyme activity	Ubc9	Yes
	Nedd4	*Nedd4*^{EY00500}	Su(+)	Ubiquitin–protein ligase activity	Neural precursor cell expressed, developmentally down-regulated 4-like (NEDD4L)	Yes
Gene transcription	CG12313	*EP(3)3367*	Su(++)	—	Carboxyl-terminal domain, RNA polymerase II, polypeptide A small phosphatase 1 (CTDSP1)	Yes
	CG6994	*EP(3)691*	Su(++)	Transcription factor activity	—	—
	emc	*emc*$^{[D]}$	NM	Transcription corepressor activity	Inhibitor of DNA binding	Yes
		emc^{03620}	Su(++)			
	CtBP			Protein C-terminus binding; transcription corepressor activity	C-terminal-binding protein 2 (CTBP2)	Yes
		CtBP^{EP3352}	Su (+)			
Nucleic acid binding	CG16940	*CG16940*^{KG02284}	E(−)	Nucleic acid binding; exoribonuclease activity	—	—
	CG9705	*CG9705*^{KG07795}	E(−)	RNA binding; nucleic acid binding	Calcium regulated heat stable protein 1, 24 kDa (CARHSP1)	Yes
	Aats-ile	*Aats-ile*^{00827}	Su(+)	RNA binding; isoleucine-tRNA ligase activity	Isoleucine-tRNA synthetase (IARS)	Yes
	danr	*P{GT1}BG01545*	E(−)	DNA binding	—	—
	dan	*EP(3)798*	Su(++)	DNA binding	—	—
Unknown functions	CG16971	*CG16971*^{EP3581}	Su(++)	—	—	—
	l(3)L3809	*l(3)L3809*^{L3809}	Su(++)	—	—	—
	CG10252	*PsEY02072*	Su(++)	—	—	—
	CG10365	*CG10365*^{KG00107}	E(−)	—	Hypothetical protein MGC4504	Yes

[a] Strengths of modification: NM, no modification; Su(++), strong suppressor; Su(+), weak suppressor; E(−), weak enhancer.
[b] Description of "Molecular Function" was adapted from FlyBase reports (http://www.flybase.net/).
[c] Based on information obtained from the NCBI UniGene database.

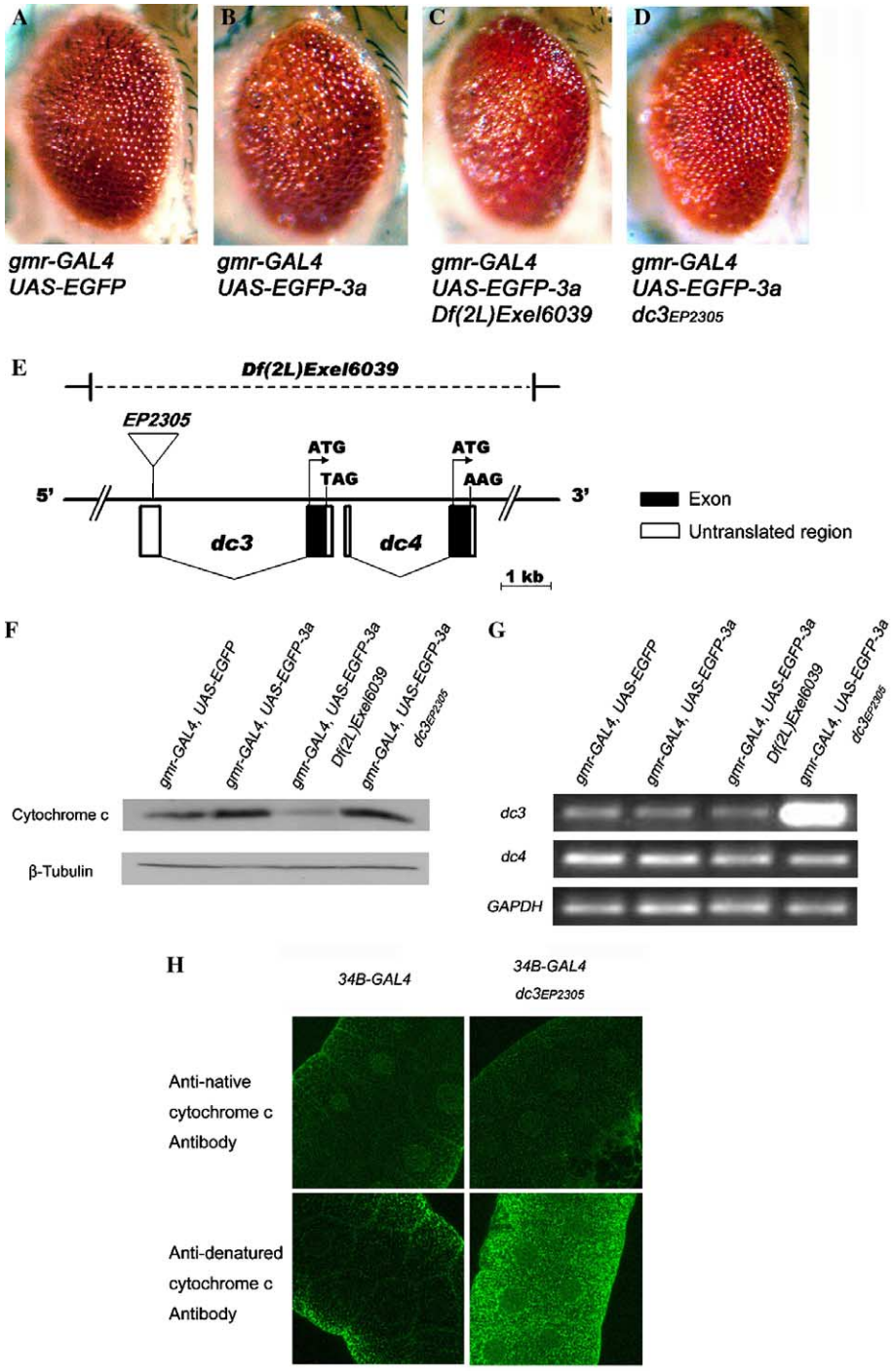

Fig. 4. Cellular cytochrome c levels correlate with *EGFP-3a*-induced rough eye phenotype in *Drosophila*. Misexpression of *EGFP-3a*, but not *EGFP* (A), caused a rough eye phenotype (B). A chromosomal deletion *Df(2L)Exel6039* of the *cytochrome c* gene region enhanced the *EGFP-3a* phenotype (C). In contrast, a *P*-element insert line, $dc3^{EP2305}$, in the *dc3* locus suppressed (D) the *EGFP-3a*-induced rough eye phenotype. (E) Genomic structure of *cytochrome c* genes in *Drosophila* shows that a *P*-element insert line, *EP2305*, is located in the 5′ untranslated region of the *dc3* locus. (F) Western blot analysis showed a significant reduction of cytochrome c protein levels in the deletion line, *Df(2L)Exel6039*. (G) RT-PCR analysis showed overexpression of the *dc3* gene in the *P*-element insert line, $dc3^{EP2305}$. (H) Immunofluorescence of cytochrome c protein in salivary gland cells. Overexpressed cytochrome c protein, via $dc3^{EP2305}$, was only detected by antibodies that recognize the denatured, but not native, cytochrome c.

of *CtBP* [28] both dominantly suppressed the *EGFP-3a* phenotype (Figs. 5C and D). It has been reported that CtBP undergoes SUMOylation and such protein posttranslational modification is mediated through an E2 ubiquitin conjugating enzyme, Ubc9 [29]. Consistent with this view, we found that a mutant allele of the fly orthologue of *Ubc9*, *lesswright* (*lwr*), showed dominant suppression of the *EGFP-3a* phenotype (Fig. 5E). It has recently been reported that *CtBP* cooperates with another transcriptional repressor, *Suppressor of Hairless Su(H)*, to determine cell fates in *Drosophila*

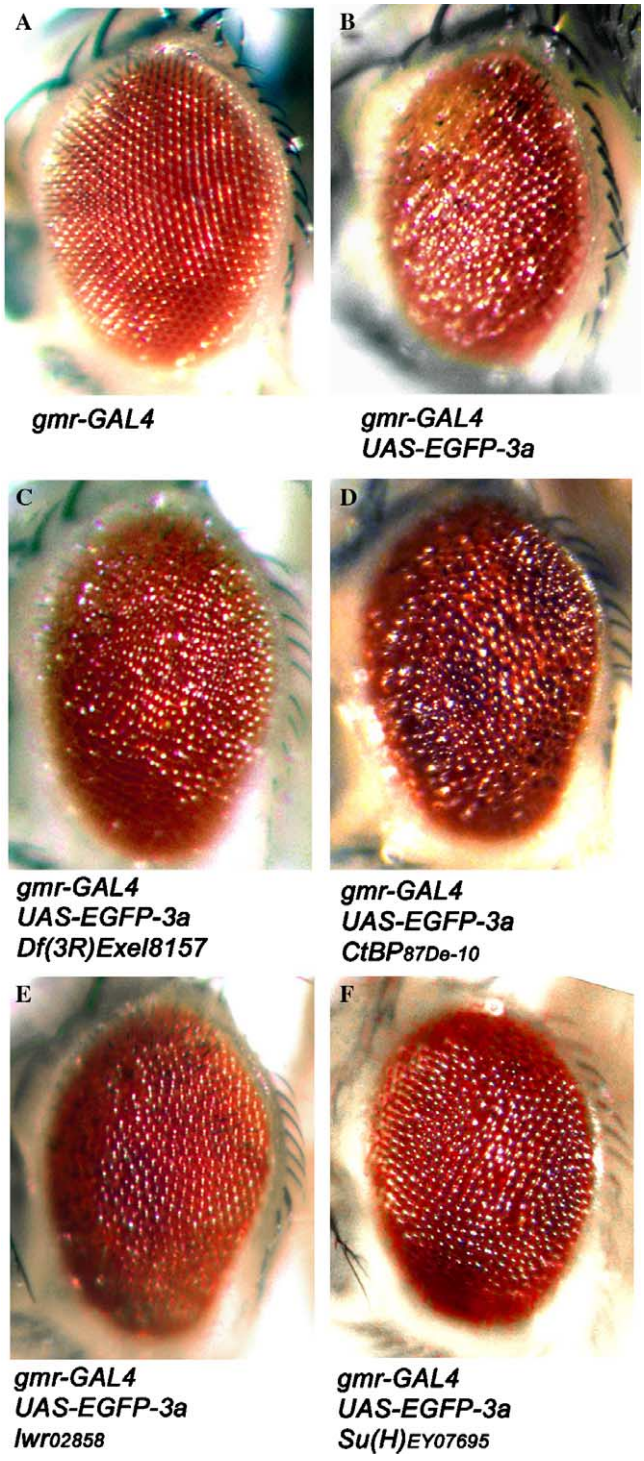

Fig. 5. *EGFP-3a* interacts with gene transcription regulatory machineries. Misexpression of the SARS-CoV *3a* gene disrupted the normal external eye structure (A; *gmr-GAL4*) and caused a rough eye phenotype in *Drosophila* (B). The *EGFP-3a*-induced rough eye phenotype was dominantly suppressed by a chromosome deletion *Df(3R)Exel8157* (C) which uncovers the 87D8-10 region, and by a null allele of *C-terminal-binding protein* ($CtBP^{87De\text{-}10}$) (D). The *EGFP-3a*-induced rough eye phenotype was suppressed by the *Ubc9* mutant *lesswright* (lwr^{02858}) which is an E2 enzyme that SUMOylates CtBP (E). A *P*-element allele of *Suppressor of hairless* ($Su(H)^{EY07695}$), inserted in the 5′ untranslated region of *Su(H)*, dominantly suppressed *EGFP-3a*-induced rough eye phenotype (F).

[30]. We further demonstrated that a mutant allele of *Su(H)* dominantly suppressed the *EGFP-3a* phenotype (Fig. 5F). Our data thus consolidate the genetic interaction of *3a* with cellular transcription machineries.

It has been shown that CtBP represses gene transcription of other transcription regulators, including the helix–loop–helix transcription regulator Id1 [31]. The *extra macrochaetae* (*emc*) gene is the *Drosophila* orthologue of *Id1* [32]. A chromosomal deletion (*Df(3L)Exel6086*) which uncovers the *emc* gene (the 61C9 region) dominantly suppressed the *EGFP-3a*-induced rough eye phenotype (Fig. 6B). Interestingly, we showed that *emc* mRNA expression level was reduced in *EGFP-3a* flies (Fig. 6D) and overexpression of *emc* suppressed the *EGFP-3a* phenotype (Fig. 6C). Our data therefore suggest that *3a* alters cellular gene transcription in vivo by interfering with transcriptional regulators including *emc*.

Discussion

Expression of the SARS-CoV 3a protein has been detected both intracellularly in infected cells [5,10] and in matured viral particles [11,12]. This indicates that 3a is a viral protein which would bear both structural [11,12] and intracellular regulatory [3,15] functions. In this study, we established a *3a* transgenic fly model and investigated the intracellular regulatory roles of *3a* in vivo. Using monoclonal antibodies against specific 3a protein sequences, we observed comparable punctate cytoplasmic expression pattern of 3a in both *Drosophila* cells (Fig. 1 and supplementary Fig. 2) and SARS-CoV-infected Vero E6 cells (supplementary Fig. 1). Similar to mammalian cells, the 3a protein was also demonstrated to undergo parallel biochemical modifications in insect cells and also became assembled into viral-like particles [12]. Altogether, these data clearly illustrate the feasibility of the use of invertebrate insect model systems to investigate functional roles of *3a*.

3a and endocytosis

The YXXΦ tetra-peptide motif is essential for the rapid internalization of proteins from the plasma membrane [13]. The 3a protein possesses such conserved YXXΦ motif (160–163 a.a.) and has been shown to be able to mediate specific internalization of 3a-specific IgG molecules to the cell interior from the culture medium [3]. Therefore, 3a has therefore been suggested to play some roles in protein trafficking in viral-infected cells [3,15]. Here, we provided genetic evidence to support a trafficking role of 3a and further linked it to clathrin-mediated endocytosis (Fig. 2). Eps15 has been shown to play an important role in the endocytosis of TfR, a cellular YXXΦ-containing protein [33]. Nedd4 is an E3 ubiquitin ligase and has also been implicated in endocytosis and virus budding [34]. Nedd4 is able to monoubiquitinate Eps15 for its endocytic function [23]. We showed that mutant alleles of both *Eps15* and *Nedd4* dominantly

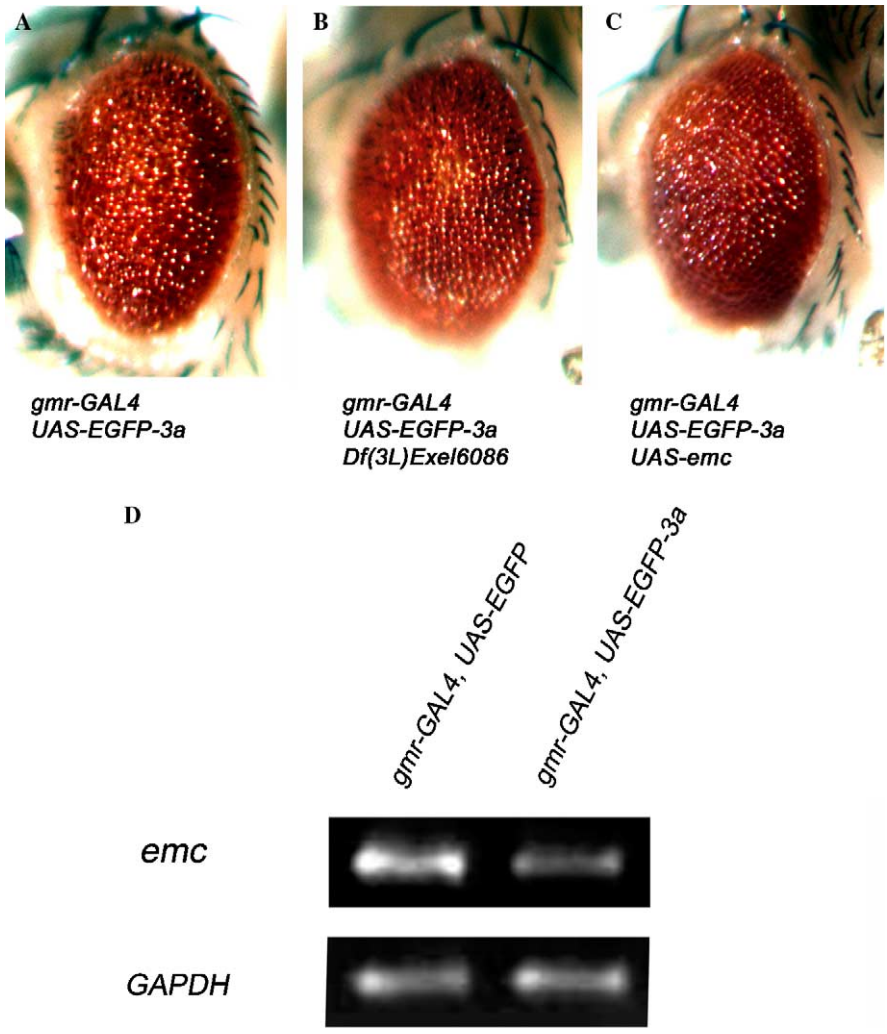

Fig. 6. *extra macrochaetae* dominantly modifies *EGFP-3a*-induced rough eye phenotype. Misexpression of *EGFP-3a* caused a rough eye phenotype (A). A chromosomal deletion *Df(3L)Exel6086* which uncovers the *extra macrochaetae* (*emc*) genomic region 61C9 (B), and an *UAS-emc* line (C) showed dominant suppression of the *EGFP-3a* phenotype. (D) RT-PCR analysis showed misexpression of *EGFP-3a* caused down-regulation of *emc* gene transcription.

suppressed the *EGFP-3a* phenotype (Fig. 2). Our data therefore support that 3a is functionally related to clathrin-mediated endocytosis. Given the physical interaction between 3a and other viral proteins (the S protein in particular, [6]), our results underscore the role of *3a* in the intracellular trafficking of SARS-CoV proteins during the viral life cycle. In humans, both Eps15 and Nedd4 are expressed in the human lung (http://www.ncbi.nlm.nih.gov/entrez/query.fcgi?db=unigene). This further highlights the functional relevance of these proteins to SARS-CoV pathogenesis.

3a is pro-apoptotic

We have recently shown that *3a* induces apoptotic cell death in Vero E6 cells [35]. Here, we demonstrated the pro-apoptotic properties of *3a* in vivo in our transgenic model (Fig. 3). We further showed that *3a*-induced apoptosis can be suppressed by coexpression of anti-apoptotic genes including the inhibitor of apoptosis protein (IAP) *DIAP1* (Figs. 3F and L), and the caspase inhibitor *P35* (Figs. 3E and K). Interestingly, upregulation of gene expression of an IAP family protein, BIRC3, was also observed in SARS-CoV-infected cells [36]. Consistent with our findings that overexpression of the caspase inhibitor *P35* suppressed the *EGFP-3a*-induced rough eye phenotype, caspase activation was also observed when *3a* was expressed in Vero E6 cells [35].

Cytochrome c plays key roles in apoptosis via the mitochondrial pathway [37]. Since cytochrome c is a potent *3a* modifier (Fig. 3), our data would suggest that *3a* induces apoptosis through the mitochondria. Suppression of the *EGFP-3a* phenotype was observed when cytochrome c was overexpressed (Fig. 4D). Interestingly, we could only detect the overexpressed cytochrome c protein in the $dc3^{EP2305}$ line with antibodies that recognize the denatured, but not native, cytochrome c proteins (Fig. 4H). This indicates that the overexpressed cytochrome c protein was not in its native conformation. It has previously been reported that overexpression of the non-native apocytochrome c (cytochrome c protein without the heme group) can block

apoptosis in mammalian cells [38]. We therefore reasoned that the $dc3^{EP2305}$ dominant suppression of the *EGFP-3a* phenotype is the result of the inhibition of apoptosis. Consistent with this view, we also observed reduced numbers of AO-positive apoptotic cells when *EGFP-3a* was coexpressed with $dc3^{EP2305}$ (Fig. 3M).

3a alters gene transcription

We found that loss-of-function of *CtBP*, a transcriptional repressor, dominantly suppressed the *EGFP-3a*-induced rough eye phenotype (Figs. 5C and D). Similar to *CtBP*, we showed that two other transcriptional regulators *Su(H)* and *emc* also dominantly suppressed the *EGFP-3a* phenotype (Figs. 5 and 6F) Further, *CtBP* has been shown to repress transcription of an *emc* orthologue, *Id1*, in mammalian cells [31]. It is therefore expected that the reduction of *CtBP* activity would lead to de-repression of *emc*. Consistent with this view, we observed suppression of the *EGFP-3a* phenotype when *emc* was overexpressed (Fig. 6C). We also observed that several EP lines (including *EP3620* and *EP0415*) that have been mapped upstream of the *emc* ORF were capable of suppressing the *EGFP-3a*-induced rough eye phenotype (data not shown).

We further showed that the mRNA expression level of *emc* was reduced in *EGFP-3a* flies (Fig. 6D). This further supports that *3a* alters gene transcription. Since *emc* is a transcriptional regulator, down-regulation of its expression would in turn affect the expression of downstream *emc*-responsive genes. It has also recently been shown that *3a* altered gene expression in cultured cells [39]. Interestingly, transcriptional alteration of some of the *3a* modifiers identified in our study (e.g., *DIAP1* and *emc*) has also been detected in SARS-CoV-infected cells [36,40]. However, we found that *3a* does not affect gene expression level of all *3a* modifiers. For example, we did not detect any alteration of *dc3* mRNA expression in *EGFP-3a* flies (Fig. 4G). This would suggest that *3a* is a multi-functional protein which affects multiple cellular processes.

In summary, we established and characterized a *Drosophila* transgenic model for the SARS-CoV *3a* gene. To investigate the intracellular roles of *3a*, we performed a genetic screen to isolate dominant *3a* modifier genes. Our data indicate that *3a* interacts genetically with multiple cellular machineries (Table 1). We further highlighted that *3a* is functionally related to clathrin-mediated endocytosis (Fig. 2) and its misexpression causes apoptosis (Figs. 3 and 4). Besides, *3a* also interacts genetically with various transcriptional regulators (Fig. 5) and it alters cellular transcription activity (Fig. 6). This is the first example illustrating the use of transgenic fly models to investigate the functional roles of *3a* and other SARS-CoV viral gene products in vivo.

Acknowledgments

We thank Erich Buchner, Jose de Celis, Shigeo Hayashi, Konrad Zinsmaier, and the Bloomington *Drosophila* Stock Center for antibodies and fly stocks; Susan Zusman for the generation of transgenic lines. We thank Patrick Law, Ben Chan, Parry Lee, and Philip Yeung for technical support; Cahir O'Kane, Tony Ip, and members of the LDR for critical comments on the manuscript. This work was supported, in part, by grants from the Health, Welfare and Food Bureau of Hong Kong (Research Fund for the Control of Infectious Diseases; 02040302); the Research Grants Council of Hong Kong (Special Competitive Earmarked Grant for SARS Research; CUHK4536/03M); and the Faculty of Medicine, CUHK (SARS Research Supplementary Grant: 6901535).

Appendix A. Supplementary data

Supplementary data associated with this article can be found, in the online version, at doi:10.1016/j.bbrc.2005.09.098.

References

[1] M.A. Marra, S.J. Jones, C.R. Astell, R.A. Holt, A. Brooks-Wilson, Y.S. Butterfield, J. Khattra, J.K. Asano, S.A. Barber, S.Y. Chan, A. Cloutier, S.M. Coughlin, D. Freeman, N. Girn, O.L. Griffith, S.R. Leach, M. Mayo, H. McDonald, S.B. Montgomery, P.K. Pandoh, A.S. Petrescu, A.G. Robertson, J.E. Schein, A. Siddiqui, D.E. Smailus, J.M. Stott, G.S. Yang, F. Plummer, A. Andonov, H. Artsob, N. Bastien, K. Bernard, T.F. Booth, D. Bowness, M. Czub, M. Drebot, L. Fernando, R. Flick, M. Garbutt, M. Gray, A. Grolla, S. Jones, H. Feldmann, A. Meyers, A. Kabani, Y. Li, S. Normand, U. Stroher, G.A. Tipples, S. Tyler, R. Vogrig, D. Ward, B. Watson, R.C. Brunham, M. Krajden, M. Petric, D.M. Skowronski, C. Upton, R.L. Roper, The Genome sequence of the SARS-associated coronavirus, Science 300 (2003) 1399–1404.

[2] P.A. Rota, M.S. Oberste, S.S. Monroe, W.A. Nix, R. Campagnoli, J.P. Icenogle, S. Penaranda, B. Bankamp, K. Maher, M.H. Chen, S. Tong, A. Tamin, L. Lowe, M. Frace, J.L. DeRisi, Q. Chen, D. Wang, D.D. Erdman, T.C. Peret, C. Burns, T.G. Ksiazek, P.E. Rollin, A. Sanchez, S. Liffick, B. Holloway, J. Limor, K. McCaustland, M. Olsen-Rasmussen, R. Fouchier, S. Gunther, A.D. Osterhaus, C. Drosten, M.A. Pallansch, L.J. Anderson, W.J. Bellini, Characterization of a novel coronavirus associated with severe acute respiratory syndrome, Science 300 (2003) 1394–1399.

[3] Y.J. Tan, E. Teng, S. Shen, T.H. Tan, P.Y. Goh, B.C. Fielding, E.E. Ooi, H.C. Tan, S.G. Lim, W. Hong, A novel severe acute respiratory syndrome coronavirus protein, U274, is transported to the cell surface and undergoes endocytosis, J. Virol. 78 (2004) 6723–6734.

[4] A.D. Singh, D. Gupta, S. Jameel, Bioinformatic analysis of the SARS virus X1 protein shows it to be a calcium-binding protein, Curr. Sci. 86 (2004) 842–844.

[5] C.J. Yu, Y.C. Chen, C.H. Hsiao, T.C. Kuo, S.C. Chang, C.Y. Lu, W.C. Wei, C.H. Lee, L.M. Huang, M.F. Chang, H.N. Ho, F.J. Lee, Identification of a novel protein 3a from severe acute respiratory syndrome coronavirus, FEBS Lett. 565 (2004) 111–116.

[6] R. Zeng, R.F. Yang, M.D. Shi, M.R. Jiang, Y.H. Xie, H.Q. Ruan, X.S. Jiang, L. Shi, H. Zhou, L. Zhang, X.D. Wu, Y. Lin, Y.Y. Ji, L. Xiong, Y. Jin, E.H. Dai, X.Y. Wang, B.Y. Si, J. Wang, H.X. Wang, C.E. Wang, Y.H. Gan, Y.C. Li, J.T. Cao, J.P. Zuo, S.F. Shan, E. Xie, S.H. Chen, Z.Q. Jiang, X. Zhang, Y. Wang, G. Pei, B. Sun, J.R. Wu, Characterization of the3a protein of SARS-associated coronavirus in infected vero E6 cells and SARS patients, J. Mol. Biol. 341 (2004) 271–279.

[7] M. Guan, H.Y. Chen, S.Y. Foo, Y.J. Tan, P.Y. Goh, S.H. Wee, Recombinant protein-based enzyme-linked immunosorbent assay and

immunochromatographic tests for detection of immunoglobulin G antibodies to severe acute respiratory syndrome (SARS) coronavirus in SARS patients, Clin. Diagn. Lab. Immunol. 11 (2004) 287–291.
[8] M. Qiu, Y. Shi, Z. Guo, Z. Chen, R. He, R. Chen, D. Zhou, E. Dai, X. Wang, B. Si, Y. Song, J. Li, L. Yang, J. Wang, H. Wang, X. Pang, J. Zhai, Z. Du, Y. Liu, Y. Zhang, L. Li, J. Wang, B. Sun, R. Yang, Antibody responses to individual proteins of SARS coronavirus and their neutralization activities, Microbes Infect. (2005).
[9] Y.J. Tan, P.Y. Goh, B.C. Fielding, S. Shen, C.F. Chou, J.L. Fu, H.N. Leong, Y.S. Leo, E.E. Ooi, A.E. Ling, S.G. Lim, W. Hong, Profiles of antibody responses against severe acute respiratory syndrome coronavirus recombinant proteins and their potential use as diagnostic markers, Clin. Diagn. Lab. Immunol. 11 (2004) 362–371.
[10] X. Yuan, J. Li, Y. Shan, Z. Yang, Z. Zhao, B. Chen, Z. Yao, B. Dong, S. Wang, J. Chen, Y. Cong, Subcellular localization and membrane association of SARS-CoV 3a protein, Virus Res. 109 (2005) 191–202.
[11] N. Ito, E.C. Mossel, K. Narayanan, V.L. Popov, C. Huang, T. Inoue, C.J. Peters, S. Makino, Severe acute respiratory syndrome Coronavirus 3a protein is a viral structural protein, J. Virol. 79 (2005) 3182–3186.
[12] S. Shen, P.S. Lin, Y.C. Chao, A. Zhang, X. Yang, S.G. Lim, W. Hong, Y.J. Tan, The severe acute respiratory syndrome coronavirus 3a is a novel structural protein, Biochem. Biophys. Res. Commun. 330 (2005) 286–292.
[13] I.S. Trowbridge, J.F. Collawn, C.R. Hopkins, Signal-dependent membrane protein trafficking in the endocytic pathway, Annu. Rev. Cell Biol. 9 (1993) 129–161.
[14] C. Schwegmann-Wessels, M. Al-Falah, D. Escors, Z. Wang, G. Zimmer, H. Deng, L. Enjuanes, H.Y. Naim, G. Herrler, A novel sorting signal for intracellular localization is present in the S protein of a porcine coronavirus but absent from severe acute respiratory syndrome-associated coronavirus, J. Biol. Chem. 279 (2004) 43661–43666.
[15] Y.J. Tan, The severe acute respiratory syndrome (SARS)-coronavirus 3a protein may function as a modulator of the trafficking properties of the spike protein, Virol. J. 2 (2005) 5.
[16] P.A. Battaglia, S. Zito, A. Macchini, F. Gigliani, A *Drosophila* model of HIV-Tat-related pathogenicity, J. Cell Sci. 114 (2001) 2787–2794.
[17] F. Leulier, C. Marchal, I. Miletich, B. Limbourg-Bouchon, R. Benarous, B. Lemaitre, Directed expression of the HIV-1 accessory protein Vpu in *Drosophila* fat-body cells inhibits Toll-dependent immune responses, EMBO Rep. 4 (2003) 976–981.
[18] P.A. Battaglia, D. Ponti, V. Naim, S. Venanzi, R. Psaila, F. Gigliani, The HIV-Tat protein induces chromosome number aberrations by affecting mitosis, Cell Motil. Cytoskeleton 61 (2005) 129–136.
[19] D. Chen, M. Wang, S. Zhou, Q. Zhou, HIV-1 Tat targets microtubules to induce apoptosis, a process promoted by the pro-apoptotic Bcl-2 relative Bim, EMBO J. 21 (2002) 6801–6810.
[20] C.R. Spresser, K.A. Carlson, *Drosophila melanogaster* as a complementary system for studying HIV-1-related genes and proteins, J. Neurosci. Res. 80 (2005) 451–455.
[21] B.A. Hay, D.A. Wassarman, G.M. Rubin, *Drosophila* homologs of baculovirus inhibitor of apoptosis proteins function to block cell death, Cell 83 (1995) 1253–1262.
[22] H. Tang, S.B. Rompani, J.B. Atkins, Y. Zhou, T. Osterwalder, W. Zhong, Numb proteins specify asymmetric cell fates via an endocytosis- and proteasome-independent pathway, Mol. Cell. Biol. 25 (2005) 2899–2909.
[23] S. Polo, S. Sigismund, M. Faretta, M. Guidi, M.R. Capua, G. Bossi, H. Chen, P. De Camilli, P.P. Di Fiore, A single motif responsible for ubiquitin recognition and monoubiquitination in endocytic proteins, Nature 416 (2002) 451–455.
[24] T. Mizutani, S. Fukushi, M. Murakami, T. Hirano, M. Saijo, I. Kurane, S. Morikawa, Tyrosine dephosphorylation of STAT3 in SARS coronavirus-infected Vero E6 cells, FEBS Lett. 577 (2004) 187–192.
[25] T. Mizutani, S. Fukushi, M. Saijo, I. Kurane, S. Morikawa, Importance of Akt signaling pathway for apoptosis in SARS-CoV-infected Vero E6 cells, Virology 327 (2004) 169–174.
[26] T. Mizutani, S. Fukushi, M. Saijo, I. Kurane, S. Morikawa, Phosphorylation of p38 MAPK and its downstream targets in SARS coronavirus-infected cells, Biochem. Biophys. Res. Commun. 319 (2004) 1228–1234.
[27] H. Yan, G. Xiao, J. Zhang, Y. Hu, F. Yuan, D.K. Cole, C. Zheng, G.F. Gao, SARS coronavirus induces apoptosis in Vero E6 cells, J. Med. Virol. 73 (2004) 323–331.
[28] S. Barolo, T. Stone, A.G. Bang, J.W. Posakony, Default repression and Notch signaling: Hairless acts as an adaptor to recruit the corepressors Groucho and dCtBP to Suppressor of Hairless, Genes Dev. 16 (2002) 1964–1976.
[29] M.H. Kagey, T.A. Melhuish, D. Wotton, The polycomb protein Pc2 is a SUMO E3, Cell 113 (2003) 127–137.
[30] B. Castro, S. Barolo, A.M. Bailey, J.W. Posakony, Lateral inhibition in proneural clusters: cis-regulatory logic and default repression by Suppressor of Hairless, Development 132 (2005) 3333–3344.
[31] X. Lin, Y.Y. Liang, B. Sun, M. Liang, Y. Shi, F.C. Brunicardi, Y. Shi, X.H. Feng, Smad6 recruits transcription corepressor CtBP to repress bone morphogenetic protein-induced transcription, Mol. Cell. Biol. 23 (2003) 9081–9093.
[32] J. Garrell, J. Modolell, The *Drosophila* extra macrochaetae locus, an antagonist of proneural genes that, like these genes, encodes a helix–loop–helix protein, Cell 61 (1990) 39–48.
[33] A. Benmerah, V. Poupon, N. Cerf-Bensussan, A. Dautry-Varsat, Mapping of Eps15 domains involved in its targeting to clathrin-coated pits, J. Biol. Chem. 275 (2000) 3288–3295.
[34] L. Hicke, Protein regulation by monoubiquitin, Nat. Rev. Mol. Cell. Biol. 2 (2001) 195–201.
[35] P.T.W. Law, C.H. Wong, T.C.C. Au, C.P. Chuck, S.K. Kong, P.K.S. Chan, K.F. To, A.W.I. Lo, J.Y.W. Chan, Y.K. Suen, H.Y.E. Chan, K.P. Fung, M.M.Y. Waye, J.J.Y. Sung, Y.M. Lo, S.K.W. Tsui, The 3a protein of severe acute respiratory syndrome-associated coronavirus induces apoptosis in Vero E6 cells, J. Gen. Virol. 86 (2005) 1921–1930.
[36] B.S. Tang, K.H. Chan, V.C. Cheng, P.C. Woo, S.K. Lau, C.C. Lam, T.L. Chan, A.K. Wu, I.F. Hung, S.Y. Leung, K.Y. Yuen, Comparative host gene transcription by microarray analysis early after infection of the Huh7 cell line by severe acute respiratory syndrome Coronavirus and human Coronavirus 229E, J. Virol. 79 (2005) 6180–6193.
[37] B.M. Polster, G. Fiskum, Mitochondrial mechanisms of neural cell apoptosis, J. Neurochem. 90 (2004) 1281–1289.
[38] A.G. Martin, H.O. Fearnhead, Apocytochrome *c* blocks caspase-9 activation and Bax-induced apoptosis, J. Biol. Chem. 277 (2002) 50834–50841.
[39] Y.J. Tan, P.Y. Tham, D.Z. Chan, C.F. Chou, S. Shen, B.C. Fielding, T.H. Tan, S.G. Lim, W. Hong, The severe acute respiratory syndrome coronavirus 3a protein up-regulates expression of fibrinogen in lung epithelial cells, J. Virol. 79 (2005) 10083–10087.
[40] J. Cinatl Jr., G. Hoever, B. Morgenstern, W. Preiser, J.U. Vogel, W.K. Hofmann, G. Bauer, M. Michaelis, H.F. Rabenau, H.W. Doerr, Infection of cultured intestinal epithelial cells with severe acute respiratory syndrome coronavirus, Cell. Mol. Life Sci. 61 (2004) 2100–2112.